

# Supplementary for "Adaptive Seasonal-Trend Decomposition for Streaming Time Series Data with Transitions and Fluctuations in Seasonality"

Thanapol Phungtua-eng ✉ and Yoshitaka Yamamoto

Department of Informatics, Shizuoka University, Shizuoka, Japan  
thanapol@yy-lab.info, yyamamoto@inf.shizuoka.ac.jp

## 1 Sliding Discrete Fourier transform (SDFT)

Here, this is proof for SDFT eq. (as shown in Eq. (2) in the main paper) [4, 5].  
Given an input sequence with a length of at least  $(N + q + 1)$ , where  $q$  denotes  
the starting index of the DFT window, we consider a DFT of length  $N$  for the  
window  $(x_q, x_{q+1}, \dots, x_{q+N-1})$ :

$$X_q = \sum_{n=0}^{N-1} x_{n+q} e^{-j2\pi nk/N} \quad (1)$$

Then, sliding to the next window with the starting point at the  $(q+1)$ -th position,  
we compute the DFT of length  $N$  for this new window  $(x_{q+1}, x_{q+2}, \dots, x_{q+N})$ ,  
dynamically tracking changes in the frequency domain as the window advances:

$$X_{q+1} = \sum_{n=0}^{N-1} x_{n+q+1} e^{-j2\pi nk/N} \quad (2)$$

Substituting  $p = n + 1$  for the range 1 to  $N$ , we have:

$$X_{q+1} = \sum_{p=1}^N x_{p+q} e^{-j2\pi(p-1)k/N} \quad (3)$$

Adjusting for the  $N$ -th term by subtracting and adding the  $p = 0$  case:

$$X_{q+1} = \sum_{p=0}^{N-1} x_{p+q} e^{-j2\pi(p-1)k/N} + x_{q+N} e^{-j2\pi(N-1)k/N} - x_q e^{j2\pi k/N} \quad (4)$$

The exponential terms can be factored as follows:

$$X_{q+1} = e^{j2\pi k/N} \left[ \sum_{p=0}^{N-1} x_{p+q} e^{-j2\pi pk/N} + x_{q+N} e^{-j2\pi Nk/N} - x_q \right] \quad (5)$$

18 The  $e^{-j2\pi Nk/N}$  term simplifies to  $1 + j0$  for  $k$  is always integer values, since  
 19  $e^{-j2\pi Nk/N} = 1$ , leading to:

$$X_{q+1} = e^{j2\pi k/N} \left[ \sum_{p=0}^{N-1} x_{p+q} e^{-j2\pi pk/N} + x_{q+N} - x_q \right] \quad (6a)$$

$$= e^{j2\pi k/N} \left[ \sum_{n=0}^{N-1} x_{n+q} e^{-j2\pi nk/N} + x_{q+N} - x_q \right] \quad (6b)$$

$$= e^{j2\pi k/N} [X_q + x_{q+N} - x_q] \quad (6c)$$

20 Note that the summation enclosed in square brackets in Eq. (6a) represents  
 21 the DFT calculated for the  $k$ th component, using  $p$  as the indexing variable  
 22 rather than  $n$ . For the latest timestamp  $t$ , the DFT results from the current slid-  
 23 ing window  $(x_{t-N+1}, \dots, x_t)$  and the previous sliding window  $(x_{t-N}, \dots, x_{t-1})$   
 24 are denoted as  $\mathcal{F}_t$  and  $\mathcal{F}_{t-1}$ , respectively. This notation allows us to succinctly  
 25 express the DFT update formula, transitioning from  $\mathcal{F}_{t-1}$  to  $\mathcal{F}_t$  as follows:

$$\mathcal{F}_t(k) = e^{j2\pi k/N} [\mathcal{F}_{t-1}(k) + x_t - x_{t-N}] \quad (7)$$

## 26 2 Spectral Peak Location Estimation

27 Spectral peak location estimation interpolates index  $k_{peak}$ , which corresponds  
 28 to the largest power in the Fourier transform result without an increase in  $N$   
 29 [6]. The  $k_{peak}$  is determined by  $k_{peak} = \hat{k} + \delta$ , where  $\hat{k}$  denotes the index of  
 30 the peak location from  $\mathcal{P}(k)$ , and  $\delta$  denotes the residual frequency that can be  
 31 positive or negative, as shown in Fig. 1. Spectral peak location estimation base  
 32 on the curve-fitting technique. This supplementary report presents a compari-  
 33 son between the non-estimator and the hybrid Aboutanios-Mulgrew and q-shift  
 34 estimator (HAQSE), which is utilized in our ASTD.

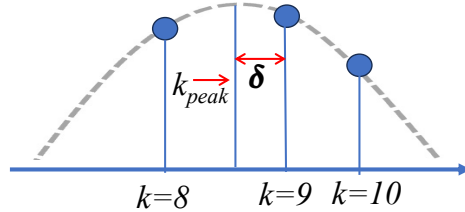


Fig. 1: Example of DFT coefficients resolution issue.

## 2.1 HAQSE

In this study, we utilize the HAQSE to determine  $k_{peak}$  from  $\mathcal{P}(k)$  [8]. HAQSE is iterative estimator that operates at a computational cost of  $O(N)$ . The HAQSE algorithm processes the results of  $\mathcal{P}(k)$  as follows:

1. **Peak Identification:** The peak index ( $\hat{k}$ ) from  $\mathcal{P}(k)$  is identified using  $\hat{k} = \operatorname{argmax}_k(\mathcal{P}(k))$ .
2. **Initial  $\delta_\alpha$  Calculation:** The initial value of  $\delta_\alpha$  is calculated according to:

$$\delta_\alpha = \frac{N}{2\pi} \arcsin \left( \sin \left( \frac{\pi}{N} \right) \Re \left\{ \frac{X_{\hat{k}+0.5} + X_{\hat{k}-0.5}}{X_{\hat{k}+0.5} - X_{\hat{k}-0.5}} \right\} \right), \quad (8)$$

where  $\Re\{\cdot\}$  denotes the real part, and  $X_k$  denotes Fourier transform for non-integer  $k$  values to accommodate fine-grained frequency estimation.

3. **Final  $\delta$  Estimation:** The final  $\delta$  is estimated using:

$$\delta = \frac{1}{c(q)} \left( \Re \left\{ \frac{X_{\hat{k}+\delta_\alpha+q} + X_{\hat{k}+\delta_\alpha-q}}{X_{\hat{k}+\delta_\alpha+q} - X_{\hat{k}+\delta_\alpha-q}} \right\} \right) + \delta_\alpha, \quad (9)$$

with  $q = \frac{1}{\sqrt[3]{N}}$  and  $c(q) = \frac{1-\pi q \cot(\pi q)}{q \cos^2(\pi q)}$ .

4. **Frequency Estimation:**  $k_{peak}$  is estimated as  $\hat{k} + \delta$ . The actual frequency, which is the peak value of  $\mathcal{P}(k)$ , is computed as  $f_{peak} = k_{peak}/N$ .

Here,  $X_k = \sum_{n=0}^{N-1} x_n \exp(-j2\pi nk/N)$  extends  $k$  to non-integer values, including  $\hat{k} \pm 0.5$ , and  $\hat{k} + \delta_\alpha \pm q$ , enabling HAQSE to estimate the actual frequency with higher resolution than possible with DFT's integer frequency bins. This method efficiently identifies  $k_{peak}$  by leveraging HAQSE's computational advantages, notably its  $O(N)$  computation cost, which is attributed to the transformation from the time domain to the frequency domain using the twiddle factor in steps 2 and 3.

## 2.2 Comparison between None-estimator and HAQSE

We conducted an evaluation with a synthetic data set consisting of a sine wave with a season length of 50 instances and a total length of 500 instances. The evaluation process began with calculating  $\mathcal{P}(k)$  using the data within a window, followed by identifying  $\hat{k} = \operatorname{argmax}_k(\mathcal{P}(k))$ . This evaluation structured the analysis into two distinct groups.

1. **Non-estimator:** we take the reciprocal with  $\hat{k}/N$  to get the season length.
2. **HAQSE estimator:** we find  $k_{peak}$  using HAQSE estimator. Then, we take the reciprocal with  $k_{peak}/N$  to get the season length.

64 The results are shown in Fig. 2, where the  $x$ -axis represents the window sizes  
 65 and the  $y$ -axis represents the season length results provided by the estimator. No-  
 66 tably,  $N$  is considered to be the optimal window size for accurately determining  
 67  $k_{peak}$  if  $N$  divided by a positive integer  $k_{peak}$  equals 50. This condition ensures  
 68 the most accurate determination of the peak frequency without the estimator.

69 The season length determined by the non-estimator is unstable and often  
 70 diverges significantly from the ground truth. However, using the optimal window  
 71 size can provide the correct season length, which exactly matches the ground  
 72 truth. HAQSE exhibited stable results without the influence of the window size.  
 73 Therefore, we used HAQSE to avoid the problem of the influence of the window  
 74 size.

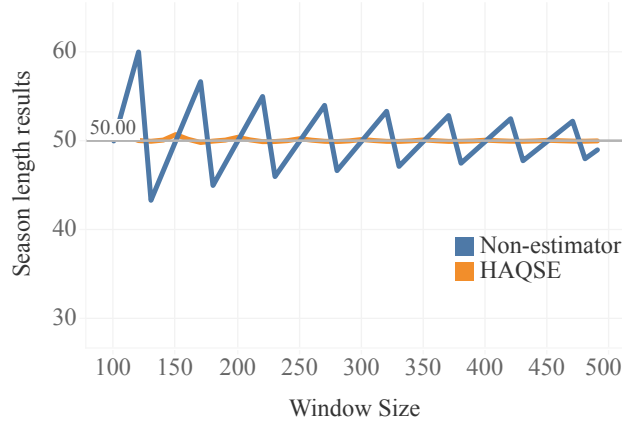


Fig. 2: Utilizing HAQSE estimator

### 75 3 Experimental Metrics for Real-world Datasets

76 This section provides additional details on the metrics used in our experiment  
 77 on real-world datasets.

78 **Trend Smoothness:** Measures the smoothness of the trend component via the  
 79 standard deviation of its first-order difference [7]. Given the trend component de-  
 80 noted by  $T = (T_0, T_1, \dots, T_t)$ , the first-order difference of the trend component,  
 81  $(\Delta T_i)$ , is calculated as:

$$\Delta T_i = T_{i+1} - T_i \quad \text{for } i = 0, 1, \dots, t-1, \quad (10)$$

82 where  $t$  denotes the latest timestamp, indicating the total length of the trend  
 83 component data. The smoothness measure, denoted as  $(\sigma_{\Delta T})$ , is then the stan-  
 84 dard deviation of these first-order differences:

$$\sigma_{\Delta T} = \sqrt{\frac{1}{t-1} \sum_{i=0}^{t-1} (\Delta T_i - \mu_{\Delta T})^2} \quad (11)$$

where  $\mu_{\Delta T}$  is the mean of the first-order differences of trend component.  
Lower values of  $\sigma_{\Delta T}$  idenote smoother trends.

**Seasonality Presence:** Measures the presence of seasonality by applying the Kruskal–Wallis test to the seasonal component [2]. Given the seasonal component denoted by  $S = (S_0, S_1, \dots, S_t)$ , the Kruskal–Wallis test statistic is calculated as:

$$W = \frac{12}{N(N+1)} \sum_{j=1}^g \frac{U_j^2}{n_j} - 3(N+1) \quad (12)$$

where  $N$  denotes the length of  $S$ ,  $g$  denotes the number of groups,  $n_j$  denotes the number of observations in the  $j$ -th group, and  $U_j$  denotes the sum of ranks in the  $j$ -th group. To determine the number of groups ( $g$ ), it is set equal to the season length  $m$ , which reflects the position within the cycle [2]. For example, if we have monthly data spanning one year (with a season length of 12), we group the data into 12 groups, with each group corresponding to one month within the cycle. Therefore, we group the observations by month, starting with January as the first group, February as the second, and so on until December, which is the twelfth group. This aligns with the season length  $m$ .

To illustrate the calculation of the sum of ranks ( $U_j$ ) within each group for the Kruskal–Wallis test, consider an example with three groups, resulting in each group having its unique set of data points:

- Group 1 ( $j = 1$ ): 5, 3, 8
- Group 2 ( $j = 2$ ): 7, 6, 2
- Group 3 ( $j = 3$ ): 4, 9, 1

Ranks are assigned to the original observations within each group, and  $U_j$ , the sum of ranks in the  $j$ -th group, is calculated:

- $U_1$  for Group 1:  $5 + 3 + 8 = 16$
- $U_2$  for Group 2:  $7 + 6 + 2 = 15$
- $U_3$  for Group 3:  $4 + 9 + 1 = 14$

Thus,  $U_j$  denotes the sum of ranks within each group. The values are  $U_1 = 16$ ,  $U_2 = 15$ , and  $U_3 = 14$ . After calculating the Kruskal–Wallis test statistic  $W$ , it is compared against a chi-square distribution with  $g - 1$  degrees of freedom. The resulting p-value is used to determine the statistical significance of the observed test statistic. Lower values suggest stable repeating cycles, indicating consistent seasonality, whereas higher values may indicate inconsistency in the seasonal component.

118 **Randomness:** Measures randomness in the residual component by applying the  
 119 Ljung-Box test to the residual component [3, 2]. Given the residual component  
 120 denoted by  $R = (R_0, R_1, \dots, R_t)$ , the Ljung-Box test statistic is calculated as:

$$Q = N(N+2) \sum_{k=1}^h \frac{\hat{\rho}_k^2}{N-k} \quad (13)$$

121 where  $N$  denotes the length of  $R$ ,  $h$  is the number of lags being tested, and  
 122  $\hat{\rho}_k$  is the autocorrelation at lag  $k$ .  $\hat{\rho}_k$  is calculated as:

$$\hat{\rho}_k = \frac{\sum_{i=0}^{N-1-k} (R_i - \mu_R)(R_{i+k} - \mu_R)}{\sum_{i=0}^{N-1} (R_i - \mu_R)^2} \quad (14)$$

123 where  $\mu_R$  denotes the the mean of the residual component ( $R$ ). To determine  
 124  $h$ , it is set to  $\min(2m, N/5)$ , where  $m$  is the season length [3]. Lower values  
 125 suggest that the residual component originates from independent and identically  
 126 distributed (iid) data, indicating the successful extraction of the seasonal  
 127 component.

128 Note that the source code for the Kruskal–Wallis and Ljung-Box tests is  
 129 available in ‘evaluation/02\_Real1\_dataset/’ [1].

## 130 References

- 131 1. Supplementary website, <https://sites.google.com/view/astd-ecmlpkdd>
- 132 2. Bee Dagum, E., Bianconcini, S.: Linear Filters Seasonal Adjustment Methods: Cen-  
 133 sus Method II and Its Variants, pp. 79–114. Springer International Publishing, Cham  
 134 (2016)
- 135 3. Hyndman, R., Athanasopoulos, G.: Forecasting: principles and practice, 2nd edition.  
 136 OTexts (2018)
- 137 4. Jacobsen, E., Lyons, R.: The sliding DFT. IEEE Signal Processing Magazine **20**(2),  
 138 74–80 (2003)
- 139 5. Jacobsen, E., Lyons, R.: An update to the sliding DFT. IEEE Signal Processing  
 140 Magazine **21**(1), 110–111 (2004)
- 141 6. Jacobsen, E., Kootsookos, P.: Fast, accurate frequency estimators. IEEE Signal Pro-  
 142 cessing Magazine **24**(3), 123–125 (2007)
- 143 7. Mishra, A., Sriharsha, R., Zhong, S.: OnlineSTL: Scaling time series decomposition  
 144 by 100x. VLDB **15**(7), 1417–1425 (2022)
- 145 8. Serbes, A.: Fast and efficient sinusoidal frequency estimation by using the DFT  
 146 coefficients. IEEE Transactions on Communications **67**(3), 2333–2342 (2019)